Revisiting photoisomerization in fluorinated analogues of acetylacetone trapped in cryogenic matrices

Alejandro Gutiérrez-Quintanilla, Michèle Chevalier, Rasa Platakyté, Justinas Ceponkus, Claudine Crépin

REVISITING PHOTOISOMERIZATION IN FLUORINATED ANALOGUES OF ACETYLACETONE TRAPPED IN CRYOGENIC MATRICES

Alejandro Gutiérrez-Quintanilla,[a,b,c,*] Michèle Chevalier,[a], Rasa Platakyté,[d] Justinas Ceponkus [d], Claudine Crépin[a,*]

[a]Université Paris-Saclay, CNRS, Institut des Sciences Moléculaires d'Orsay, 91405, Orsay, France.
[b]Instituto Superior de Tecnologías y Ciencias Aplicadas (InSTEC), Universidad de La Habana. Ave. Salvador Allende No. 1110, Plaza de la Revolución, La Habana 10400, Cuba.
[c]Université de Pau et des Pays de l'Adour, E2S UPPA, CNRS, IPREM, Pau, France
[d]Institute of Chemical Physics, Vilnius University, Vilnius, Lithuania
* a.gutierrez-quintanilla@univ-pau.fr

Abstract

UV-induced processes are commonly studied in acetylacetone analogues. In this contribution, we revisit the existing work on the photoisomerization process in some of the fluorinated analogues of acetylacetone, i.e., trifluoroacetylacetone (F3-acac) and hexafluoroacetylacetone (F6-acac). We performed selective UV laser excitation of these molecules trapped in soft cryogenic matrices, namely neon and *para*-hydrogen, and probed by vibrational spectroscopy. Clear spectroscopy of 3 isomers of F6-acac and 6 isomers of F3-acac, is obtained, including the first characterization of a second open enol isomer of hexafluoroacetylacetone. In addition, we present the electronic absorption spectra of both molecules in cryogenic matrices before and after specific UV irradiations, giving new data on the electronic transitions of photoproducts. Vibrational and electronic experimental results are analyzed and discussed within comparisons with DFT and TD-DFT calculations. Our findings contribute to a deeper understanding of the photoisomerization process in these molecules after electronic excitation in gas and condensed phase.

1. Introduction

Hexafluoroacetylacetone ($C_5O_2F_6H_2$) and trifluoroacetylacetone ($C_5O_2F_3H_5$) are two halogenated analogues of acetylacetone ($C_5O_2H_8$) where either one or both methyl groups (CH_3) are substituted by trifluoromethyl groups (CF_3), see Figure 1. As in acetylacetone, the tautomeric equilibrium allows the presence of two isomeric forms: keto and enol, although, in the gas phase, the enol isomer is largely preponderant. The presence of a Resonance Assisted Hydrogen Bond (RAHB) in this family of molecules largely stabilizes the chelated or "close" enol isomer (referred to as CCC) compared to any other "open" enolic isomers. The latter are formed by rotations around the C_1-C_2 and C_2-C_3 backbone "ring" bonds and the C_3-OH bond.

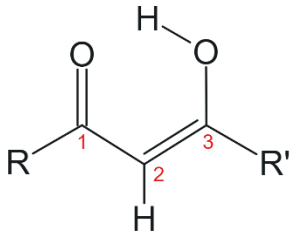

Fig. 1 Scheme of the molecular structure of the enolic form of the two studied β-diketones: F6-acac (R=R'= CF_3) and F3-acac (R= CH_3, R'= CF_3 or R=CF_3, R'=CH_3). The combination of *cis* (C) and *trans* (T) configurations around the C_1-C_2, C_2=C_3 and C_3-O bonds produces eight XYZ isomers, where X, Y, and Z can be C or T, e.g., the one shown corresponds to CCC (also known as chelated or close enolic form)

After acetylacetone (acac), hexafluoroacetylacetone (F6-acac) is one of the best-studied β-diketones regarding its structure and spectroscopy. Initial studies carried out by Andreassen *et al.* [1] and Iijima *et al.* [2] using gas-phase electron diffraction (GED) suggested the presence of the enol isomer with a structure near the C_2 or C_{2v} symmetries. But, more recent experimental and theoretical works concluded that in the gas phase, the pseudo-cycle of the molecule has a planar geometry with C_s symmetry [3–6]. All these works also show a weakening of the intramolecular hydrogen bond (IHB) in F6-acac compared to acac.

The vibrational spectrum of this analogue has been previously obtained in gas, liquid, and solid phases [7]. The electronic spectra in the gas and liquid phases are also known [8]. Nakata's group has extended these works by obtaining the infrared and UV absorption spectra in an argon matrix [9, 10]. In these two papers, the photophysics of the molecule in argon matrix by means of a combination of broadband and 10 nm bandwidth UV irradiation was also studied. The results showed the production of a new "open" enol isomer after UV irradiation. To date, these two works are the only ones developed in cryogenic matrices for F6-acac [9, 10]. Like acetylacetone, UV irradiation in the gas phase and in supersonic jets leads to photofragmentation instead of isomerization [11–13]. The absence of fluorescence suggests a very fast non-radiative process that dominates the dynamics of the molecule after electronic excitation. Indeed, a recent work by Haugen et al. shed light on one of the deexcitation steps involved [14]. The use of ultrafast X-ray transient absorption spectroscopy allowed them to observe an ultrafast intersystem crossing between $S_1 \rightarrow T_1$, with a possible presence of various configurational isomers in both states [14]. In addition, the comparison of the work of Haugen et al. [14] with a previous one on acetylacetone [15], shows that the total fluorination of methyl groups in acetylacetone does not significantly alter the intersystem crossing rate between the S_1 and T_1 states.

Besides, trifluoroacetylacetone (F3-acac) is an intermediate structure between acetylacetone and hexafluoroacetylacetone. Because of the presence of two different terminal substituents (CF_3 and CH_3), it can have in principle two different forms or tautomers in the enol isomer depending on whether the hydroxyl group is on the CH_3 or the CF_3 side, see Figure 1. The corresponding enol isomers

will be named hereafter XYZ(CO) and XYZ(OH) respectively, by defining the position of the CF_3 group on the C=O side or the O-H one of the molecule. For instance, CCC(CO) and CCC(OH) are used for the chelated enols. The structure of this molecule has been analyzed with experimental and theoretical approaches. Like hexafluoroacetylacetone the first attempts to describe its structure in the gas phase, by using information from GED experiments, concluded that the internal "ring" has a local C_{2v} symmetry [1]. A similar structure with some degree of asymmetry for the ring and a *syn* position for the CF_3 was obtained by Gordon and Koob using INDO (Intermediate Neglect of Differential Overlap) molecular orbital theory [16]. Subsequent works using DFT and MP2 theoretical methods and vibrational or microwave experimental information have supported the asymmetric structure, with almost C_s symmetry, and with the hydroxyl group on the CH_3 side in the most stable isomer [5, 17–19]. In a recent work of our group, combining theoretical calculations and experimental vibrational spectroscopies, we showed that the C_s symmetry reproduces the IR and Raman spectra obtained in different cryogenic matrices and that both chelated enols were detected in the spectra (including gas phase spectra), the less stable one (CCC(OH)) being present as traces in the cryogenic samples [20].

The vibrational spectra (infrared and Raman) of this analogue were studied also by Tayyari *et al.* and Raissi *et al.* in the solution and gas phases [7, 17, 21]. An infrared study in argon matrix was carried out by Minoura *et* al [22], following the works previously reported in acetylacetone and hexafluoroacetylacetone. The authors confirmed the C_s structure previously proposed and reported UV irradiation of trifluoroacetylacetone as in the previous studies on acetylacetone and hexafluoroacetylacetone. Four open enol isomers of F3-acac were observed after irradiation [22]. Like in the case of hexafluoroacetylacetone and acetylacetone, UV irradiation of trifluoroacetylacetone in the gas phase provokes fragmentation instead of isomerization [13].

In this family of molecules, understanding the electronic excitation and subsequent relaxation processes, which include photoisomerization pathways, can be important not only from a fundamental perspective but also in applications related to UV photoprotective systems such as sunscreens. Despite the efforts already developed to understand the vibrational spectrum and the photophysics of these compounds, there are still some open questions to address, especially concerning the processes to get open isomers and the selectivity in the stabilized open isomers. Taking Nakata's work and our own work on acetylacetone as a reference point, we should expect more "open" (non-chelated) isomers formed in F6-acac after UV irradiation than the one observed in the work carried out by Nakata's group on argon matrix. As previously demonstrated for acetylacetone isotopologues (hydrogenated and partially deuterated), XYC-XYT pairs of isomers differing only in the O-H orientation, are expected to be produced in cryogenic solids when this family of molecules relaxes back to the S_0 ground state after the initial S_2 excitation. A subsequent conversion in the ground state through hydrogen tunneling may

take place, leaving only the most stable isomer of each pair [23]. In the case of F3-acac, Minoura et al, found that both CTT-F and CTC-F (Minoura's notation) isomers are formed, the latter being only observed during irradiation and not as a stable final product, in agreement with the assumption of a tunneling process from CTT-F to CTC-F [22]. However, the matrix studies on acetylacetone clearly showed that the number of open isomers stabilized in the matrix depends on the host. Thus, we have decided to revisit the photophysics of both molecules, by using soft cryogenic hosts (*para*-hydrogen and neon matrices) and selective UV excitation of the samples using a frequency-tunable laser to explore other matrices and try to clarify the open questions. We have gathered the current experimental and theoretical data on the photophysics of this family of molecules to offer in the discussion section an updated picture of the photoexcitation processes taking place. In addition, the vibrational spectra collected in softer matrices, like neon and *para*-hydrogen, where site effects are reduced, add clear experimental data that can be used to improve the current description of C-F vibrational modes with theoretical methods. The position and intensity of these vibrational modes were still not completely well reproduced with most used theoretical methods, i.e., DFT and perturbational methods. We also performed new theoretical calculations to support the experimental results.

2. Methods

2.1. Theoretical calculations

The calculations were run using Gaussian 09 (D.01) software [24] in the GMPCS cluster (Grappe Massivement Parallèle de Calcul Scientifique) at Orsay, Université Paris-Saclay. Geometry optimizations for all the isomers of trifluoroacetylacetone and hexafluoroacetylacetone, as well as frequency calculations were performed at the Density Functional Theory (DFT) level of theory with either B3LYP [25] or M06-2X [26] functional and 6-311++G(3df,3pd) basis set [27]. The M06-2X was chosen because it has been shown that it can produce a better overall description of vibrational spectra for halogenated β-diketones than B3LYP, especially for the C-F vibrational modes [28]. However, this method always overestimates the frequencies of C=C and C=O stretching modes in the analogues of acetylacetone. A very tight convergence criterion and the -96032 integration grid were used in all calculations. Vibrational frequencies and infrared intensities were obtained within harmonic approximation. When reported in figures, each transition is represented by the convolution of the transition line with a Lorentzian function of FWHM=2 cm^{-1}. Intensities are normalized when represented in figures. Frequency calculations allow us to confirm the presence of stable optimized structures (potential energy minima) and to compute Zero-Point Energies (ZPEs) for all the structures to correct the electronic energies. A scaling factor of 0.970 (F6-acac) and 0.973 (F3-acac) was used to

partially correct the computed frequencies for the vibrational anharmonicity (main approximation). Nevertheless, the same scaling factors were used for all the explored matrices.

The theoretical electronic absorption (UV-Vis) spectra of enolic isomers were also obtained by solving the time-dependent DFT (TD-DFT) equations [29–31] according to the method implemented in Gaussian 16 (B.01) [32]. The five lowest singlet states were computed using the same functional and basis set, as described above.

The NCIplot software [33, 34] was employed to perform the noncovalent interaction (NCI) study. The .wfn output files obtained from Gaussian software after optimization calculations were used as input files for the program. NCI analysis allowed identifying the weak interactions at play in the systems of interest. In this case, the output was visualized with the Visual Molecular Dynamics program [35].

2.2. Experimental Setup

Two different matrix isolation experimental setups were used for these studies. The first one was used for nitrogen and neon (Air Liquide 6.0) matrices. 1,1,1,5,5,5-Hexafluoroacetylacetone (98%) and 1,1,1-Trifluoroacetylacetone (98%) from Sigma-Aldrich were first degassed in the vacuum system by using freeze-pump-thaw cycle and used without further purification. Sample and matrix gases were mixed in a steel vacuum system with their ratios estimated by using common manometric techniques. In a typical experiment, 1 mbar of the sample molecule and 1000 mbar of the matrix gas were mixed, and approximately 8-13 mmol of the mixture were deposited at a deposition rate of around 10 $mmol.h^{-1}$ onto a spectral window (cesium iodide for FT-IR measurements). This internal window (attached to the cold head) was cooled between 7.2 and 8.8 K in a closed cycle He cryostat (APD Cryogenics Inc.).

Ultraviolet spectra were acquired with this experimental setup using a 0.6 m JobinYvon grating monochromator, a CCD camera (Andor DH720), and a deuterium lamp (34500-60000 cm^{-1}) as the light source. In these experiments, sapphire was used as an internal window for the deposition of the sample.

The second setup was employed for experiments in the *para*-hydrogen (pH_2) matrix. It included two closed-cycle helium cryostats, connected by a stainless-steel tube. The first cryostat was used for the *ortho/para*-hydrogen conversion process (Air Products, Displex DE202) with Fe_2O_3 powder (Sigma-Aldrich 99 %) as a catalyst, and the other for the sample deposition (ICE: Innovative Cryogenic Engineering, RDK 415D, He Compressor: Sumitomo F-50). In the *ortho/para* conversion cryostat, the temperature was raised to 15-17K after the spin conversion at about 14 K. Then, pH_2 was sent through a stainless-steel tube to the main cryostat. A small reservoir containing the sample was attached to this tube. Two Swagelok microvalves allowed controlling the host gas flux (pH_2) and the amount of vapor from the sample. The mixture of gases arrived directly in front of the internal diamond window

(2.8 K) fixed to the cold head of the second cryostat. This cryostat was pumped by a turbomolecular pump (Oerlikon, Leybold vacuum, Turbovac 600C, pumping speed for H_2: 570 $l.s^{-1}$), which allowed reaching pressures slightly below 10^{-6} mbar at 293 K. The pH_2 converter was pumped by a diffusion pump (CIT Alcatel). A few experiments in neon were performed with this second set-up replacing H_2 with neon before the converter and maintaining the temperature of the conversion cryostat at 40 K to let a flow of neon go through. The sample-to-host gas ratio is not easy to determine a priori in this experimental configuration, due to the lack of precise control over the continuous mixing process. Different experimental runs were needed to obtain the correct deposition conditions, where only monomeric species were present in the sample (inferred from FT-IR spectra).

In both experimental setups, the IR spectra were obtained by means of an FT-IR spectrometer (Nicolet 670/870 or iS50) at a resolution of 0.5 cm^{-1}, averaging 256 scans.

UV irradiation experiments were conducted by using an OPO laser (Continuum Surelite II + Optical Parametric Oscillator, Horizon system, repetition rate: 10 Hz, pulse-duration: 4 ns, spectral width 5 cm^{-1}), operating in the 220−300 nm range with the energy around 1 mJ/pulse. IR spectra were recorded before and after each irradiation. Several irradiation cycles with different wavelength combinations were applied to the same sample.

3. Results

3.1. Hexafluoroacetylacetone

3.1.1. Theoretical results

The energy order for the isomers of hexafluoroacetylacetone at M06-2X/6-311++G(3df,3pd) level of theory is shown in Figure 2. The energy values are corrected with the Zero-Point Energy of each isomer. B3LYP calculations were also performed with the same basis set. Very similar results were obtained, observing just inversion in the relative energy order of CCT and TCC isomers on the one hand, and CTT and TCT isomers on the other hand. In these two groups of isomers, the energy difference is less than 1.5 $kJ.mol^{-1}$, which is lower than the absolute error for these methods. So, the important conclusion is that in both cases the isomers have very similar relative energies. A similar result was obtained by Nagashima et al by using B3LYP/6-31G** method [9].

Analysis of the electronic density (NCI calculation) was performed for the eight enol isomers to consider the influence of non-covalent interactions in each of the XYC-XYT pairs. The result shows that CTT and TCC isomers are the most stable ones in the CTZ and TCZ pairs because of the presence of an attractive non-covalent interaction at play between CF_3 and H-O groups (see Figure S1). It is worth mentioning that the high stability of the CCT isomer (compared to the one in acac) cannot probably be attributed to non-covalent interactions, although there could be an attractive one between the O-H

and the CF_3 groups. Both are slightly out of the main plain of the carbon skeleton. In fact, F6-acac is the only analogue of acetylacetone where this isomer is more stable than most of the rest of other open isomers [23]. As we will see later in the energy calculations for the F3-acac analogue, both CF_3 groups are needed to reach that level of stability. This indicates that electronic acceptor inductive effects on both sides are at play. This effect can reduce the electrostatic repulsion between the lone pairs of oxygen atoms in the CCT configuration. Indeed, a comparison of the partial atomic charges of both oxygens in F6-acac and acac shows a reduction of the negative charge in the former (see Table S1 in SI), as well as a longer O···O distance (2.782 vs 2.755 Å at the M06-2X/6-311++G(3df,3pd) level of theory).

Three more facts can also be noticed from our theoretical results. First, our results agree with previous studies on the β-diketone family showing that the intramolecular hydrogen bond strength changes as F6-acac < F3-acac < acac [21, 36]. This is mainly deduced from the comparison of the O···O distance and the O-H···O angle in the CCC isomer, which are longer and smaller respectively in F6-acac compared to acac (see Table S2 in SI). Second, both isomers of the TTZ pair (TTT and TTC) present a non-planar carbon-skeleton structure. This marked planarity break is not observed in other analogues of acetylacetone. This is an indication of strong repulsive effects between the two CF_3 groups in F6-acac. Finally, the position of the OH group is out of the carbon-skeleton plain of the molecule in TCC and TCT isomers (like in CCT). This change is also accompanied by a rotation of the CF_3 groups (CO side in TCC and OH side in TCT) out of the expected planar dihedral angle. This points to the presence of C-F···H-O attractive interactions favoring such geometries, which are however evidenced through NCI calculation in the case of TCC, but not in TCT (see Figure S1 in SI).

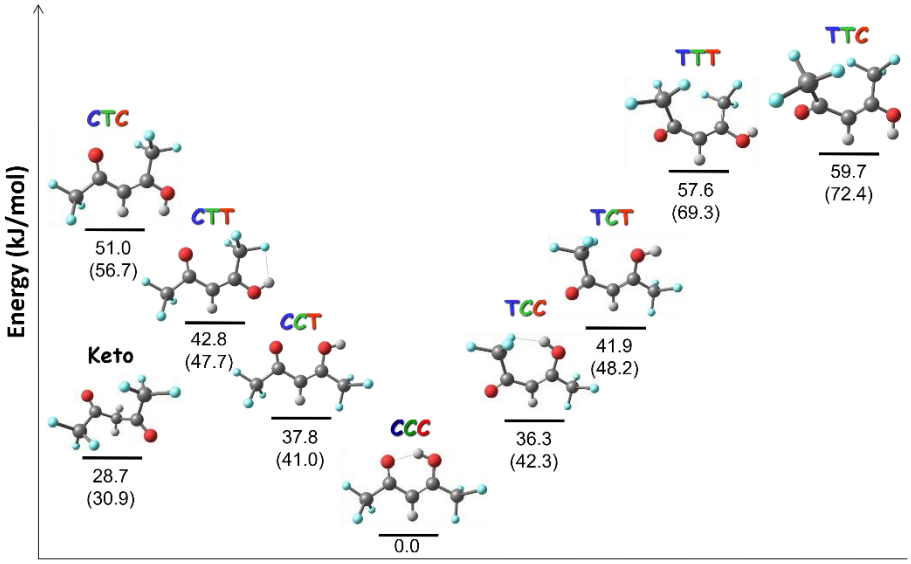

Fig. 2 ZPE corrected theoretical relative energies (kJ/mol) for hexafluoroacetylacetone (configurational and conformational) isomers w.r.t CCC isomer calculated at M06-2X/6-311++G(3df,3pd) level of theory (B3LYP in parentheses)

3.1.2. FT-IR spectra of F6-acac isolated in Ne and pH_2

The FT-IR spectra of F6-acac in (a) neon, and (b) *para*-hydrogen matrices are shown in Figure 3 for the 1800-650cm^{-1} region. The infrared spectrum calculated in the harmonic approximation for the CCC isomer in the C_s symmetry is shown in panel (c).

The comparison of the experimental and theoretical spectra confirms the presence of the CCC chelated enol isomer with a C_s symmetry. The match is very good when the M06-2X functional is used and a scaling factor of 0.970 is applied for frequencies. The B3LYP functional was also used in calculations but the agreement was not as good as with the M06-2X functional, mainly in the CF_3 stretching region (1160-1230 cm^{-1}). A deeper investigation of the performance of B3LYP and M06-2X (including scaling factor), as well as other functionals and the MP2 method, to describe the vibrational spectrum of the CCC isomer is discussed in a forthcoming publication reporting the vibrational spectra in argon matrices. The assignment of the bands is described in Table S3. Besides CCC no other enol isomer was found in the deposited sample and bands from keto tautomer were not found.

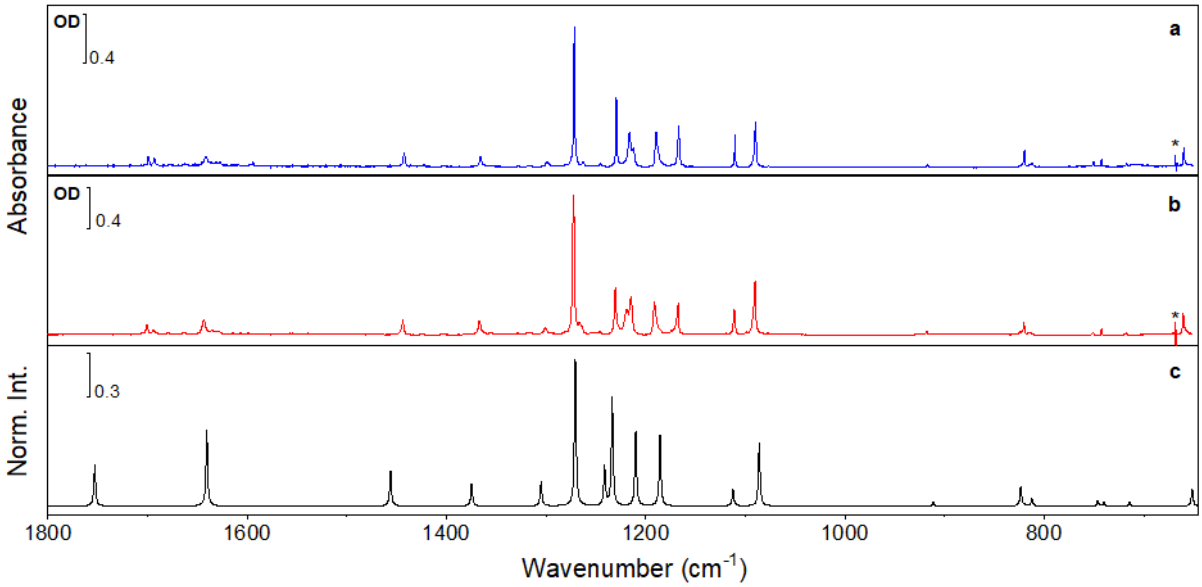

Fig. 3 FT-IR spectra of hexafluoroacetylacetone isolated in (a) *para*-hydrogen at 2.8 K and (b) neon at 8 K. (c) theoretical infrared spectrum (M06-2X) of CCC isomer in harmonic approximation with computed frequencies scaled by a 0.970 scaling factor. * Artifacts

It is interesting to notice the presence of a structure in some bands in the C=O/C=C stretching region. A careful discrimination from water bands shows that the symmetric mode at lower frequency (~1640 cm^{-1}) has some additional small sub-structures in neon and *para*-hydrogen. On the other hand, a clear doublet (~6 cm^{-1}) is observed for the antisymmetric C=O/C=C stretching band near 1695 cm^{-1} (Figure S2). A third couple of bands centered in this region around 1670 cm^{-1} is observed in both matrices with a common shift value (~16 cm^{-1}). However, these last two bands are not due to fundamental

transitions, only C=O/C=C stretching modes are expected in this region. Additional experiments performed in nitrogen matrices also show the presence of multiple bands in this region (Figure S2).

These doublets are not due to site effects because they are present even in the very soft *para*-hydrogen matrix. Moreover, the shift is the same in all the matrices, including argon and nitrogen. A closer look at the spectrum reported by Nagashima et al. [9] in argon matrix shows the presence of such multiplets, which we have also confirmed by performing our own experiments in argon matrix (forthcoming publication). From the analysis of the fundamentals in the theoretical and experimental spectrum, no overtones are expected in this region. Attempts to perform anharmonic frequency calculations to obtain possible combination bands and resonances with the VPT2 method implemented in Gaussian 16 failed even with a lower basis set (very long and resource-demanding). Because our main goal was to focus on the photoisomerization process, we have not pursued any further investigation on the structure of these bands. Unfortunately, this question remains open and cannot be answered with certainty based only on these results. One possible experimental way of answering this question is to study the deuterated isotopologues, which is out of the scope of the present research, mainly focused on the open enol isomers.

3.1.3. Electronic absorption spectra of F6-acac

The electronic absorption spectrum of this molecule was previously obtained in gas phase [8] and in argon matrix [9]. We have recorded the electronic absorption spectrum of the CCC isomer in neon matrix before performing the UV laser irradiation. The spectrum is shown in Figure S4. It is similar to the one previously obtained by Nagashima et al. in the argon matrix [9]. The broad band with some vibronic structure, near 270 nm corresponds to the CCC isomer, the only present in the deposited sample. After irradiation at wavelengths between 270-290 nm, a new absorption band with a maximum near 253 nm appears. This indicates the production of new species in the matrix. The three results are summarized in Table 1. One can notice that the UV spectra shown in Figure S4 correspond to absorption recorded in samples with different mixtures of CCC and CTT isomers, as revealed by IR spectra of the same samples.

On the other hand, the calculated wavelengths of the five lowest computed electronic transitions (TD-DFT calculations), for each of the eight isomers, are reported in Table S4. These simulations show that the main electronic absorption corresponds to the $S_2 \leftarrow S_0$ transition with $\pi \rightarrow \pi^*$ molecular orbitals involved. All other electronic transitions (in particular $S_1 \leftarrow S_0$) have very low oscillator strength and are separated by more than 60 nm from the $S_2 \leftarrow S_0$ transition (Table S4). These results reinforce the previous assignment of the experimental band and guarantee that the performed irradiations between 270-290 nm only correspond to the $S_2 \leftarrow S_0$ transition. Also, these results confirm that the chelated enol

isomer presents the lower absorption energy for this transition, with a marked redshift compared to all the open enol isomers. The theoretical shift (Δ) is consistent with the experimental one (see Table 1 and Table S3).

Table 1 Experimental and computed data (TD-DFT: M06-2X/6-311++G(3df,3pd)) on the UV spectra of matrix-isolated F3-acac: as-deposited sample (isomer CCC) and after irradiation, and the shift between them (Δ). Previous results in the gas phase [8] and argon matrix [9] are also included for comparison. Experimental bands are broad, especially after irradiation, so band positions (in nm) are approximative

	CCC	**After irradiation**	Δ
Gas phase [8]	267	-	-
Ar matrix [9]	272	249	23
Present work Ne matrix	270	253*	17
Theoretical ($S_2 \leftarrow S_0$)	246	230 (CTT) 227 (TCC)	∼18

* This value has been obtained after subtraction of the CCC spectrum (as-deposited sample)

3.1.4. UV laser irradiation: CTT and TCC isomers

Taking advantage of the knowledge of the absorption spectra before and after UV irradiation, we started the study of the infrared signature of open enol isomers by performing UV laser irradiation at longer wavelengths, near the onset of the observed UV-absorption spectrum of CCC (at 290 nm), for more than 40 minutes. Such UV irradiation should excite only CCC isomers. Next, the wavelength was gradually changed to lower wavelengths. From the beginning of the irradiation CCC infrared bands decreased in intensity while a new group of bands grew. In the CCC isomer, the experimental band due to the OH stretching mode is not observed, due to a strong intramolecular O···H-O hydrogen bond. Thus, the production of open enol isomers is evidenced by the appearance of new bands in the free OH stretching region, near 3700 cm^{-1} (the spectra in pH_2 matrix is shown as an example in Figure SS). Considering the different kinetics of the growing bands we were able to isolate two groups: one growing faster than the other when irradiating at 290 nm, and the second increasing very fast under irradiation at 265 nm. Comparison with theoretical infrared spectra of all the isomers allowed to assign these two groups to CTT (Table 2) and TCC isomers (Table 3) respectively. These isomers are two of the four lowest energy open enol isomers (see Figure 2).

The experimental spectra of CTT in *para*-hydrogen and neon matrices along with the theoretical frequency calculation for this isomer are shown in Figure 4. As for the CCC isomer the agreement between experimental and theoretical spectra is good overall. As in CCC, the C=O/C=C and CF_3 stretching regions are not completely well described, but the uncertainty is small enough to leave no

doubt about the assignment. CTT isomer was previously found to be produced in argon matrix either by irradiation from a broadband mercury lamp [9] or a narrowband light from a monochromator coupled to a Xe lamp [19], which supports our result.

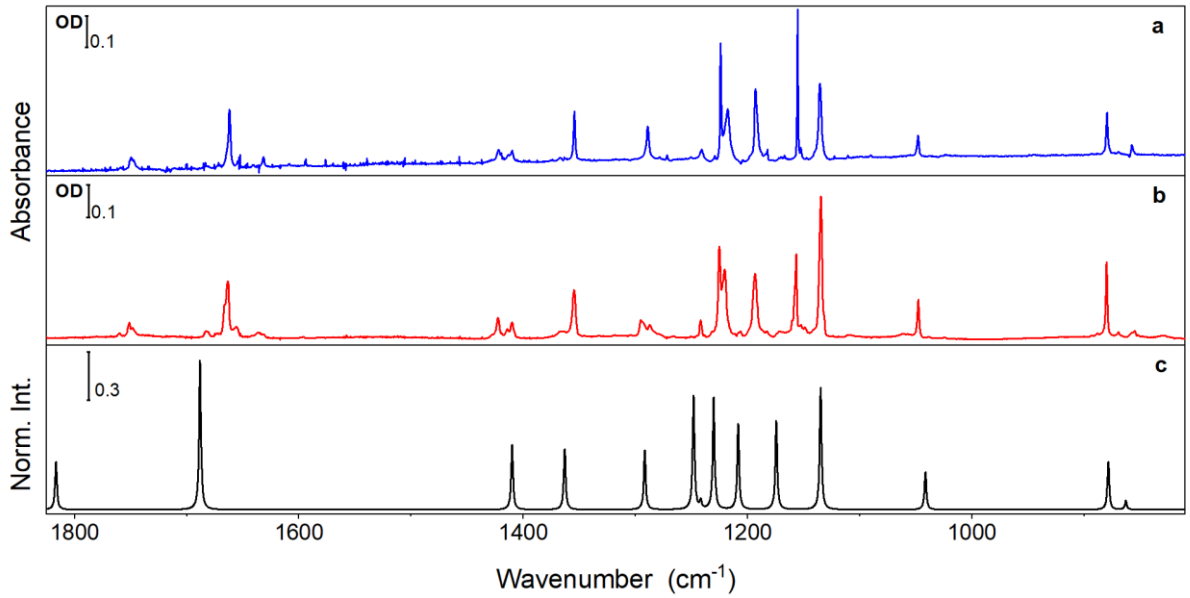

Fig. 4 Experimental FT-IR spectra of hexafluoroacetylacetone CTT isomer in (a) para-hydrogen at 2.8 K and (b) neon at 8 K. The experimental spectra are the result of subtractions of different spectra along irradiation to remove CCC and TCC bands. Panel (c) shows theoretical infrared spectrum (M06-2X) of CTT isomer in the harmonic approximation with computed frequencies scaled by 0.970

As mentioned before, another open enol isomer is produced and stabilized in the matrix after lower wavelength irradiation (265 nm). Figure 5 shows the assignment of the TCC isomer which grows faster than CTT when the 265 nm wavelength is used. The assignment of this isomer is less evident than in the case of CTT. This is mainly due to the small infrared activity (intensity) of modes other than C=O/C=C and CF_3 stretching, which as we already mentioned have the highest disagreement with theoretical results. Nevertheless, a careful comparison of all the open enol isomers allows us to suggest TCC as the isomer produced at a shorter wavelength (see Figure S4). This isomer was not found in previous studies in argon matrix [10].

Table 2 Vibrational assignment of the CTT isomer of hexafluoroacetylacetone. Infrared experimental frequencies (cm^{-1}) in neon and *para*-hydrogen matrices. Calculated harmonic frequencies [M06-2X/6-311++G(3df,3pd)] (cm^{-1}) are also included for comparison. IR (km/mol) intensities were obtained in the harmonic approximation. Scaling factor (sf): 0.970. The mode assignments given in ref. [9] do not exactly match those proposed in the present work. The complete set of calculated frequencies and intensities, as well as the corresponding assignments, is given in Table SS

Assignment (simplified description)	**Frequencies**				**Infrared Intensities**
	Experimental			**Theoretical Harmonic*sf**	
	Ar (Ref. [9])	**Ne**	**pH_2**		
vOH	3593	3612.8	3596.7	3732.5	261

νCH		3051.6	3048.8	3126.1	5
νC=O/νC=C (as)	1746	1751.7	1749.6	1816.7	124
νC=O/νC=C (s)/δOH	1663*	1663.6	1662.1	1688.3	387
δOH/δCH	1410	1422.6 1414.5 1409.8	1421.8 1413.6 1410.0	1410.0	167
νC-OH/νC-CH_3	1356*	1354.8	1354.5	1363.1	157
νCF_3 (CO side)/δOH/δCH	1290	1294.8 1286.9	1289.1	1291.7	153
νCF_3 (OH side)	1223*	1225.3	1224.0	1248.2	294
νCF_3 (both sides)/δOH/δCH	1237	1241.8	1241.0	1241.8	21
νCF_3 (CO side)/δOH/δCH	1206	1220.5	1217.8	1230.3	290
νCF_3 (OH side)/δCH	1193*	1193.5	1192.6	1208.4	221
νCF_3 (CO side)	1154	1157.1	1155.4	1174.4	231
νCF_3 (OH side)/δOH/δCH	1134*	1134.9	1135.4	1134.9	317
νC-C	1048	1047.8	1048.1	1041.5	97
νCF_3 (CO side)	881	880.0	879.5	878.4	123
γCH	855	855.5	856.9	862.7	23
$\delta_s CF_3$(OH side)	786	785.0	784.4	784.4	7
γCH/γC=O	749	747.6	747.0	749.7	5
$\delta_s CF_3$(CO side)	734*	731.7 730.2	731.6	728.8	65

[a] main characteristic motion; **ν**, stretching; **δ,** in plane bending; **γ**, out of plane bending; **s**, symmetric; **as**, antisymmetric. * Bands exhibiting splitting in argon matrix according to Ref. [9]. A grey background is used to identify multiplets

An interesting point is that the production of this second isomer is only enhanced in a very narrow range of wavelengths around 265 nm. At 268 nm CTT is mainly produced. Following excitations below 260 nm the system starts to go back to CCC, as it was also noted in the case of the argon matrix [10]. This narrow window to produce the TCC isomer could explain why it was not previously observed in the careful studies performed by Nakata's group. In the same way, our recorded UV absorption spectra do not involve samples containing TCC. The final assignment for the open enol isomers is shown in Tables 2 and 3.

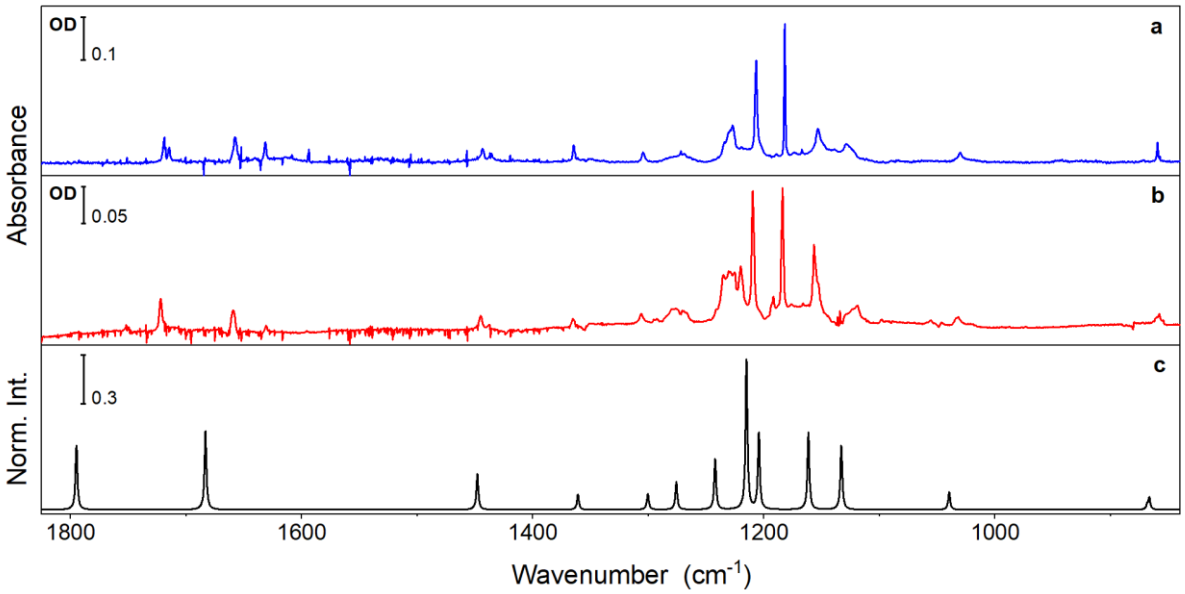

Fig. 5 Experimental spectra of TCC isomer in (a) *para*-hydrogen at 2.8 K and (b) neon at 8 K. The experimental spectra are the result of subtractions of different spectra along irradiation to remove CCC and CTT bands. Panel (c) shows theoretical frequency calculation (M06-2X) of TCC isomer in harmonic approximation with 0.970 scaling factor

Table 3 Vibrational assignment of the TCC isomer of hexafluoroacetylacetone. Infrared experimental frequencies (cm^{-1}) in neon and *para*-hydrogen matrices. Calculated harmonic frequencies [M06-2X/6-311++G(3df,3pd)] (cm^{-1}) are also included for comparison. IR (km/mol) intensities were obtained in the harmonic approximation. Scaling factor (sf): 0.970. The complete set of calculated frequencies and intensities, as well as the corresponding simplified description of the assignments, is given in Table SS2

Assignment (simplified description)	Frequencies			Infrared Intensities
	Experimental		Theoretical Harmonic*sf	
	Ne	pH_2		
vOH	3631.5	3623.7	3749.7	199
vCH	3234.4		3146.8	11
vCO	1722.1	1719.3 1714.4	1794.9	239
vC=C	1659.5	1658.0	1683.3	293
vC-OH	1445.0 1437.9	1443.5 1435.9	1448.0	134
vC-CH_3/δCH	1365.4	1364.6	1361.0	56
vC-CH_3/δOH/δCH	1306.0	1304.4	1300.5	59
vCF_3 (both sides)/δOH	1274.7	1272.3	1275.8	103
vCF_3 (both sides)/δOH	1235.4 1225.8 1219.9	1227.0	1242.2	188
vCF_3 (OH side)/δOH	1209.5	1206.8	1215.1	556
vCF_3 (OH side)	1184.0	1182.0	1204.4	283
vCF_3 (CO side)/δOH/δCH	1156.4	1153.1	1161.5	287
vCF_3 (CO side)/δOH/δCH	1119.1	1128.9	1133.1	239
vC-OH	1032.6	1030.3	1039.7	66

νC-CF₃	858.4*	859.3*	868.3	17
γCH			866.5	44
δsCF₃(CO side)	769.1		769.4	7
δsCF₃(OH side) /Δ	730.0	730.3	726.5	13

[a] main characteristic motion; **ν**, stretching; **δ,** in plane bending; **γ**, out of plane bending; **s**, symmetric; **as**, antisymmetric. A grey background is used to identify multiplets. * These two modes accidentally overlap in frequency

3.2. Trifluoroacetylacetone

3.2.1. Theoretical results

Due to unequal CF_3 and CH_3 substituents on trifluoacetylacetone the number of possible enolic isomers is twice the number found in acac and F6-acac. One set corresponds to the presence of the CF_3 group at the carbonyl (C=O) side (XYZ(CO)) and the other with the CF_3 at the hydroxyl (OH) side (XYZ(OH)). The theoretical energy order (at the M06-2X/6-311++G(3df,3pd) level of theory) relative to the most stable enol isomer is shown in Figure 6. The presence of unequal terminal substituents in F3-acac also provokes the presence of multiple stable structures in the keto tautomer with similar energies (difference of ∼0.5 - 3 kJ/mol). The one shown in Figure 6 corresponds to the lower energy structure founded by turning the dihedral angles around the C_1-C_2 and C_2-C_3 bonds.

When it comes to the enolic isomers, the first noteworthy point is the similarity in the energy order between F3-acac(OH) and F6-acac, with the main difference lying in two aspects: the relative order of the isomers in the TCC(OH)/ TCT(OH) pair, and a higher relative energy of all the other isomers in respect to CCC(OH). The higher energy of TCC(OH) isomer compared to TCC(CO), and TCC in F6-acac, can be explained by the presence in these latter of an attractive interaction between a CF_3 group and the hydrogen from the hydroxyl group, not present in the former. The same effect can also explain the exchange in energy order in the CTC-CTT pair in F3-acac(CO) when compared to F3-acac(OH) and F6-acac, where non-covalent attractive interaction are at play. The presence of such non-covalent attractive interaction is illustrated in Figure S5 for the CTT(OH) isomer. On the other hand, the higher relative energy in the CYZ isomers in F3-acac(OH) could be explained by repulsive interactions between one of the electron lone pairs of the carbonyl oxygen and the CF_3 groups (CTC(OH) and CTT(OH)) or a lone pair from hydroxylic oxygen (CCT(OH)). These effects are more evident when comparing the relative energies of these three isomers with their corresponding “C=O side” analogues. In the case of F6-acac, the presence of a second CF_3 group at the carbonyl side (C=O) impacts, by negative electronic inductive effect (-I), the electronic density at the carbonyl oxygen, tuning the interactions where this group is involved. In the same sense, a loss of symmetry (moving from C_s to C_1 point group) is also observed for some isomers in F6-acac and F3-acac, i.e. CCT, TCC and TCT in F6-acac; and TCC(CO), CCT(OH) and TCT(OH). This is mainly due to an out of symmetry plane position of the OH group involved

in the O-H···CF_3 interactions. The relevant role of these repulsive and attractive interactions in the stability of these analogues was qualitatively advanced by Minoura et al [22], and confirmed here with a higher level of theory.

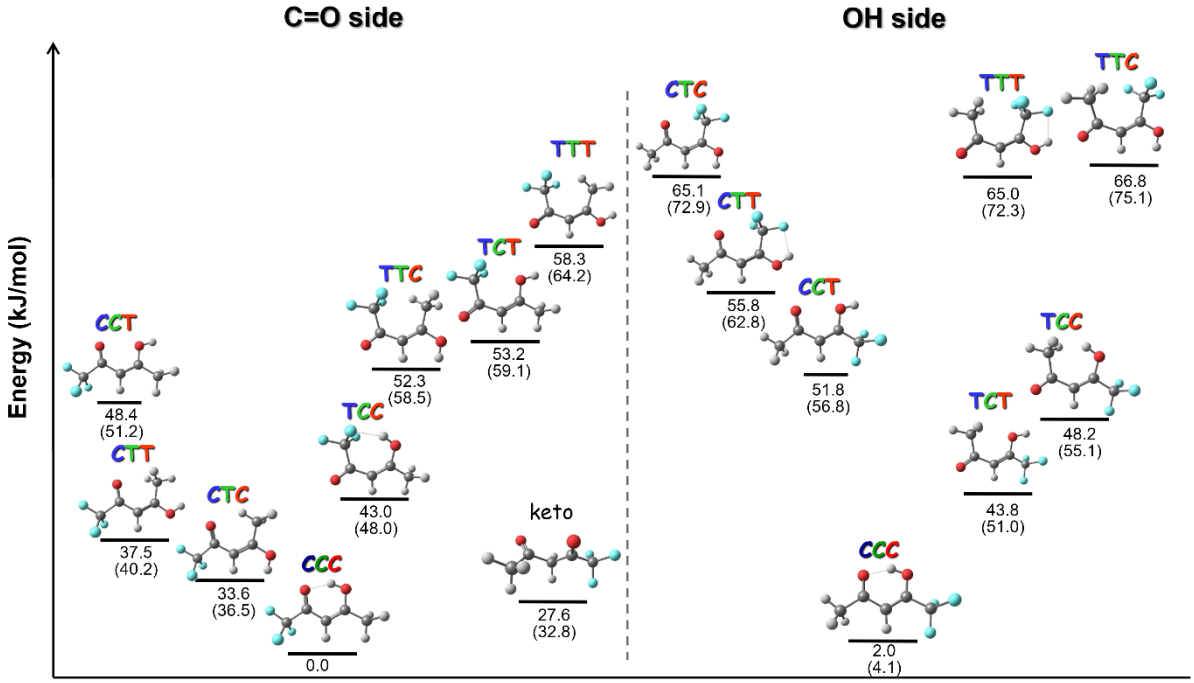

Fig. 6 Schemes and theoretical relative energies (kJ/mol) of open enol (configurational and conformational) isomers of the C=O and OH tautomers (depending on the CF_3 position) and the most stable structure found for the keto tautomer compared to the CCC(CO) isomer, in F3-acac at M06-2X/6-311++G(3df,3pd) level of theory. Zero Point Energy is included

It should be noted that the CCC(OH) tautomer is only 2.0 kJ.mol^{-1} higher in energy than the CCC(CO) isomer. In previous reports values between 3.4–5.7 kJ.mol^{-1} have been found using B3LYP/6-31G* and higher basis sets [5, 17, 22, 37]. The proton transfer barrier has also been estimated in a previous study, the obtained value was 11 kJ/mol at B3LYP/6-31G** level of theory [17]. It was previously believed that the low energetic separation between both isomers and the relatively low barrier between both implied that at low temperatures the CCC(OH) isomer will convert to CCC(CO) by tunneling effect, and that only this isomer should be observed in deposited samples [22]. However, as we demonstrate in a recent study, both chelated enol isomers are present in the deposited samples, their ratio depending on the host solid, but with a dominant presence of CCC(CO) [20].

3.2.2. FT-IR spectra of F3-acac isolated in Ne and pH_2 matrices

The experimental spectra of the deposited samples in *para*-hydrogen and neon were already published in our recent work [20], and it is shown in Figure S6. The overall spectra are close to the one obtained by Minoura *et al.* in argon matrix [22]. However, an important conclusion drawn in our previous work on F3-acac is that a small amount of the CCC(OH) isomer is present in the deposited samples along with the dominating CCC(CO) isomer, being the CCC(OH)/CCC(CO) ratio host-dependent (≤0.007 in Ne,

and ≤0.08 in pH_2)[20]. This allows us to conclude that in Ne and pH_2 matrices, the majority of effects observed after electronic excitation in deposited samples will only concern the CCC(CO) isomer. However, it should be noticed this is not the case in other matrices. Experiments in nitrogen matrix show not only a higher ratio CCC(OH)/CCC(CO) ~ 0.42, but a change in it after annealing or UV irradiation cycles.

3.2.3. Electronic absorption spectrum of F3-acac

The electronic absorption spectrum of trifluoroacetylacetone in neon matrix is shown in Figure 7 for the deposited sample and after two different irradiation sequences from two different samples: 285 + 270 nm and 260 + 245 nm. No bibliographic reference was found about the UV spectrum of this molecule.

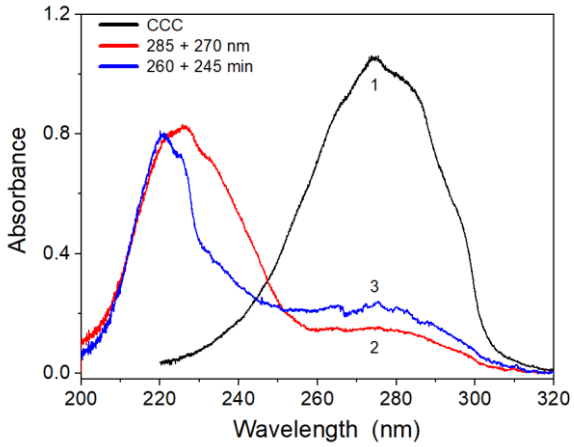

Fig. 7 Electronic absorption spectra of trifluoroacetylacetone in neon matrix: (1, black) deposited sample, mainly corresponding to the CCC(CO) isomer, (2, red) after 285 + 270 nm irradiation sequence, (3, blue) after 260 + 245 nm irradiation sequence (on a different sample under the same experimental conditions of deposition)

Like other analogues of acetylacetone, the electronic absorption spectrum of the deposited sample shows a broad band centered around 277 nm corresponding to the $\pi \rightarrow \pi^*$ transition. The band shows some broad structure. We can also remark that this transition exhibits bathochromic shift compared to acac and F6-acac. On the other hand, two other bands exhibit strong hypsochromic shift can be distinguished after the irradiation sequences shown in Figure 7. By similarity with the other β-diketones [9, 23, 38], these bands can belong to open isomers, and two groups of isomers are expected to be formed after UV irradiation. Additional evidence supports this statement. We also recorded FT-IR spectra during these experiments. Because of the use of sapphire as an optical substrate for the acquisition of the UV spectra, the accessible IR range is limited under this configuration (> 1600 cm^{-1}). Nevertheless, it permits to identify, through the ν_{OH} and ν_{CO} modes, the emergence of open enol isomers after irradiation. The assignment of these isomers is detailed in sections 3.2.5 and 3.2.6.

Theoretical results obtained through TD-DFT calculations show that the two CCC tautomers have very close absorption bands (see Table 4, and the whole set of TD-DFT results in Table S10, including oscillator strengths). This implies that the position of the CF_3 group has a small influence on the electronic properties of these specific configurations. In both tautomers, the main electronic absorption corresponds to the $S_2 \leftarrow S_0$ transition with $\pi \rightarrow \pi^*$ molecular orbitals involved. All other electronic transitions (in particular $S_1 \leftarrow S_0$) have low or very low oscillator strength and are separated by more than 50 nm from the $S_2 \leftarrow S_0$ transition (Table S10). Also, it is worth noting that the open enol isomers in F3-acac(CO) absorb at higher wavelengths compared to their F3-acac(OH) analogues (see Table S10). In consequence, the big blueshift observed in the UV absorption after irradiation is an indication that mainly F3-acac(OH) isomers are observed in the electronic spectra after the irradiation sequence employed in such experiments, as confirmed by the corresponding IR spectra recorded on the same samples after the same UV irradiations.

Table 4 Experimental and computed data (TD-DFT: M06-2X/6-311++G(3df,3pd)) on the UV spectra of matrix-isolated F3-acac: as-deposited sample (isomer CCC) and after irradiation, as well as the difference between both (Δ). Experimental bands are broad, so band positions (in nm) are approximative

	CCC	**After irradiation**	Δ
Present work Ne matrix	277	226 221	51 56
Theoretical ($S_2 \leftarrow S_0$)	239 (CO) 239 (OH)	233 (CTC(CO)) 221 (CTT(OH)) 207 (TCT(OH))	6 18 32

3.2.4. UV laser irradiation

The UV laser irradiation of F3-acac isolated in neon and *para*-hydrogen was carried out like in the case of F6-acac. Irradiation starts at a high wavelength (290 nm) placed near the onset of the electronic absorption band, and it was subsequently changed to lower values (until 230 nm). Contrary to F6-acac, the conversion of the chelated enol isomer at lower energies (270-300 nm) is more difficult even after long irradiation times, and a small residual amount of CCC is almost always present even after long irradiations. The formation of three sets of bands assigned to three open enol isomers was then observed (CTC(CO), CTT(OH), and TCT(OH)). The isomers were identified by comparison of their experimental spectra with theoretical calculations. The increase of each isomer greatly depends on the irradiation wavelength sequence used.

3.2.5. CTC(CO)

One isomer is quickly formed when UV irradiation starts (290-285 nm): CTC(CO), see Figure 8. The match with the theoretical infrared spectrum is good. Experimental and theoretical values of

vibrational modes are reported in Table 5. CTC(CO) isomer is the most stable open enol isomer of both possible sets of isomers. However, according to TD-DFT calculations (see Table S10 and Table 4), this isomer absorbs close to CCC isomers, and as experimentally observed, it is efficiently excited and converted to other isomers. It should be noted that the spectra obtained in Figure 7 correspond to longer irradiation times compared to those used in the experiments shown in Figure 8. In consequence, CTC(CO) is not observed in Figure 7 because it has been formed and already converted to another isomer.

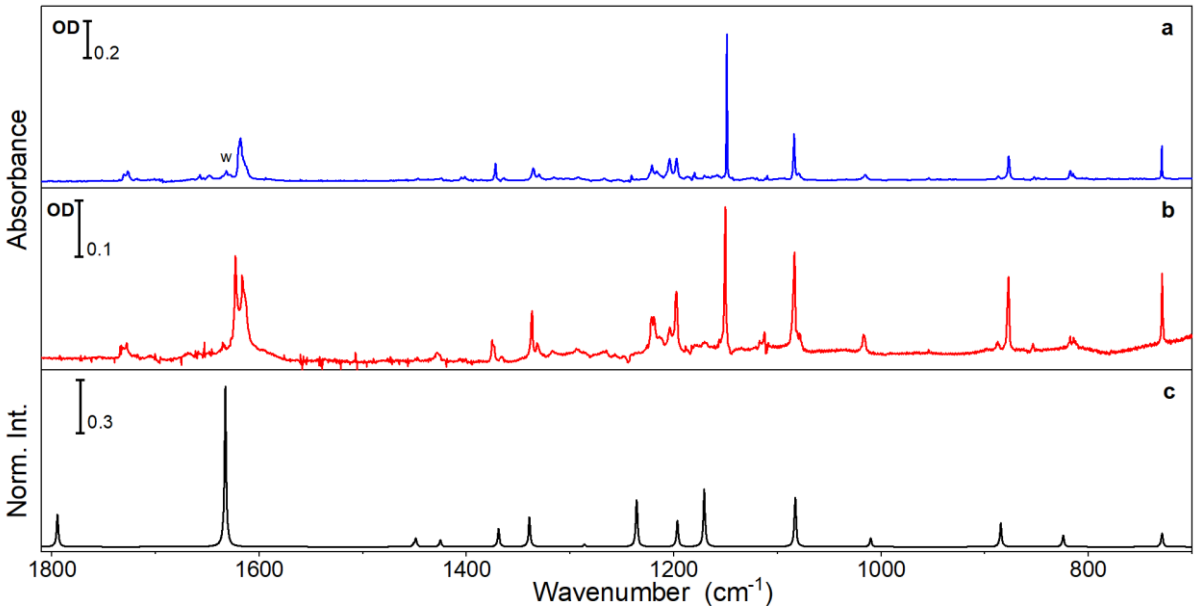

Fig. 8 Experimental infrared spectra of the CTC(CO) isomer of trifluoroacetylacetone in (a) *para*-hydrogen at 2.8 K and (b) neon at 8 K. (c) theoretical harmonic infrared spectrum, a scaling factor of 0.973 was used for frequencies. The experimental spectra are the result of subtractions of different spectra along irradiation to remove CCC and bands from other open enol isomers. w : residual water band

Table 5 Vibrational assignment of the CTC(CO) isomer of trifluoroacetylacetone. Vibrational experimental frequencies (cm^{-1}) in neon and *para*-hydrogen. Values for argon matrices from ref. [22] are also included. Calculated harmonic frequencies [M06-2X/6-311++G(3df,3pd)] (cm^{-1}) are added for comparison. IR intensities (km/mol) are obtained in the harmonic approximation. Scaling factor (sf): 0.973. The complete set of calculated frequencies and intensities, as well as the corresponding assignments, is given in Table S6

Assignments (simplified description)	Frequency			Theoretical	
	Ne	pH_2	Ar (ref. [22])	Harm.*sf(0.973)	Infrared Int.
νOH	3614.8	3597.6	3588	3751.4	76
νCH_3	3022.0			3134.8	6
νCH	2967.0			3102.8	5
νCH_3	2932.0			3046.6	1
νCH_3				2990.5	4
νC=O	1732.2 1728.3	1730.9 1727.4	1725	1794.7	148

νC=C	1623.2 1616.3	1618.5	1617	1632.8	732
δCH₃ **δCH₃/δCH/ δOH/νC-C**	1448.4*	1447.3*	1447	1451.0 1449.0	10 37
δCH₃ /νC-CH₃	1428.4	1424.5		1425.3	32
δCH₃ /νC-CF₃	1374.6	1372.4	1370	1369.2	81
νC-CF₃/δCH₃	1337.3 1331.9	1335.9 1330.2	1335	1339.4	134
νCF₃/ δCH	1293.0	1292.3		1286.0	11
νCF₃/ δCH	1221.5 1219.3	1221.3	1218	1235.9	213
δCH/ δOH	1204.2 1197.8	1204.3 1197.7	1195	1196.6	119
νCF₃	1150.5	1149.0	1147	1170.7	262
νC(H)-C(=O)/νC-CH₃/ νCF₃	1083.8	1084.0	1084	1082.9	225
ρCH₃				1039.0	1
ρCH₃	1016.6	1015.3	1014	1010.0	40
νC-CF₃	877.4	877.2	878	884.6	109
νC-CH₃	853.7	852.6		852.9	1
γCH	817.9 814.1	817.7 815.0	815	824.4	53
Γ				754.7	0.0
δsCF₃	729.1	729.4	731	729.0	61

[a] main characteristic motion; **ν**, stretching; **δ,** in plane bending; **γ**, out of plane bending; **ρ**, in plane rocking; **Γ**: out of plane carbon skeleton deformation; **s**, symmetric; **as**, antisymmetric. A grey background is used to identify multiplets. * These two modes accidentally overlap in frequency

3.2.6. CTT(OH) and TCT(OH)

The second group of isomers is produced from the beginning of the irradiation at 285 nm. This group appears very fast when CTC(CO) isomer is irradiated at 270 nm or the CCC isomer is directly irradiated with 260 nm wavelength from the beginning. Two isomers were identified in this group. Different ratios between the two isomers are obtained depending on the irradiation sequence used.

The spectra in neon and *para*-hydrogen matrices are shown in Figure 9 and Figure 10. The isomers are CTT(OH) and TCT(OH) respectively. In both cases, the match with theoretical calculation is quite good. Experimental and theoretical values of vibrational modes are reported in Table 6 and Table 7. The biggest disagreement is observed in the 1300-1100 cm^{-1} region like in F6-acac. Both isomers are the most stable species of their XYC-XYT pairs (see Figure 6).

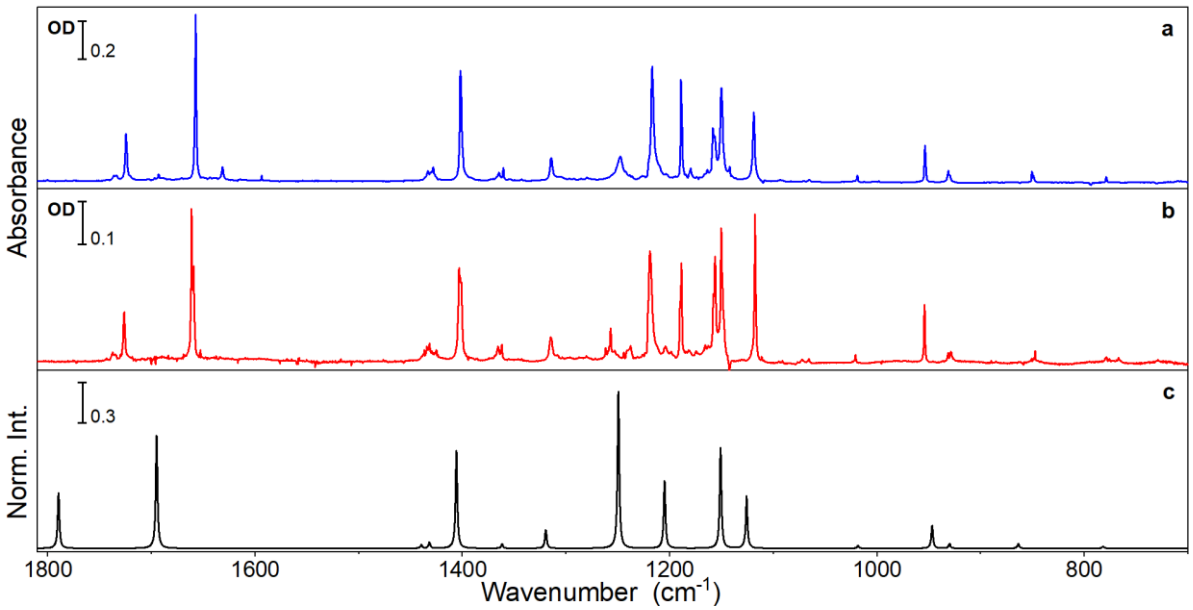

Fig 9 Experimental infrared spectra of the CTT(OH) isomer of trifluoroacetylacetone in (a) *para*-hydrogen at 2.8 K and (b) neon at 8 K. (c) theoretical harmonic infrared spectrum, a scaling factor of 0.973 was used for frequencies. The experimental spectra are the result of subtractions of different spectra along irradiation to remove CCC and bands from other open enol isomers

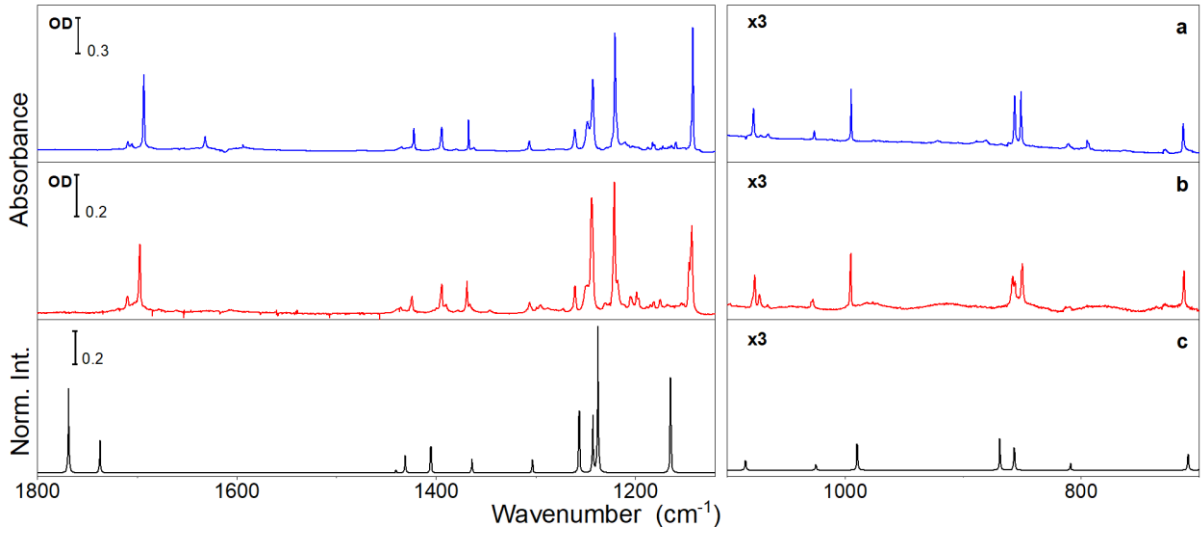

Fig. 10 Experimental infrared spectra of the TCT(OH) isomer of trifluoroacetylacetone in (a) *para*-hydrogen at 2.8 K and (b) neon at 8 K. (c) theoretical harmonic infrared spectrum, a scaling factor of 0.973 was used for frequencies. The experimental spectra are the result of subtractions of different spectra along irradiation to remove CCC and bands from other open enol isomers. A three-times vertical zoom (x3) has been applied in the right panel

No other stable isomer was detected. We observed the same set of isomers as obtained by Minoura *et al.* [22] in argon matrix. The formation of a transient isomer CTT(CO) was observed during the irradiation process in their work. We did not perform such kind of measurement because of experimental constraints to obtain quality IR spectra and to perform UV irradiations at the same time. We detected slightly more vibrational bands of open isomers in the soft matrices we used. Our results, combined with those from Minoura et al., highlight the fact that the studied cryogenic hosts (pH_2, Ne, Ar) seem to have no influence on isomer production.

Thanks to the IR identification of the enol isomers, the UV absorption profiles obtained after UV irradiation (red and blue curves in Figure 7) are assigned to samples containing either a mixture of CTT(OH) and TCT(OH) (red curve) or TCT(OH) as the main open isomer (blue curve). This result agrees with TD-DFT results showing TCT(OH) as the detected open isomer with the highest-energy S_2-S_0 electronic transition (Table 4).

Table 6 Vibrational assignment of the CTT(OH) isomer of trifluoroacetylacetone in neon and *para*-hydrogen. Values for argon matrices from ref. [22] are also included. Calculated harmonic frequencies [M06-2X/6-311++G(3df,3pd)] (cm-1) are added for comparison. IR intensities (km/mol) are obtained in the harmonic approximation. Scaling factor (sf): 0.973. The complete set of calculated frequencies and intensities, as well as the corresponding assignments, is given in Table S7

Assignments (simplified description)	**Frequencies**				**Infrared Intensities**
	Experimental			**Theoretical Harmonic*sf**	
	Ne	**pH_2**	**Ar (ref.** [22]**)**		
νOH	3626.1	3613.5	3610	3758.1	233
νCH				3121.0	2
νCH_3	3031.5	3030.9 3022.6		3098.9	5
νCH_3	2970.9	2966.1		3042.8	3
νCH_3		2923.6		2980.6	1
νC=O/ νC=C	1726.6	1714.7	1726	1789.8	151
νC=C/ νC=O/ δOH	1661.4 1659.4	1657.5	1659	1695.1	308
δCH_3	1434.5 1431.9	1433.5		1439.6	9
δCH_3	1429.5 1425.3	1428.3	1427	1431.8	16
δOH/ δCH/ $\nu C\text{-}CF_3$/ δCH_3	1403.3 1402.4 1401.2	1402	1400	1405.9	265
δCH_3/ $\nu C\text{-}CH_3$	1365.7 1362.3	1365.1 1360.7	1360	1361.7	12
δCH_3/δOH/ $\nu C\text{-}CF_3$/ νC(H)-C(=O)	1314.8	1314.6	1315	1319.6	50
νCF_3/ δOH	1219.1	1217.2	1214	1249.7	268
δOH/ δCH	1239.4	1248	1252	1249.5	160
νCF_3/ δCH	1190.1 1188.8	1189	1189	1205.1	184
δCH/ ρCH_3	1156.5 1150.5	1157.4 1150.3	1149	1151.0	273
δOH/ νCF_3/ρCH_3	1117.7	1119.0	1118	1125.9	142
ρCH_3	1021	1019.1	1017	1018.2	7
ρCH_3	954.4	953.8	954	946.9	62

ρCH₃/νC(H)-C(=O)	931.5 928.8	931.5 930.0	931	930.0	13
γCH/Γ	847.6	850.6 849.1	850	863.6	12
νC-CF₃/δCF₃	779.0	778.8	779	781.3	6
Γ		676.5		685.1	2
Δ		653.9	656	650.7	14

[a] main characteristic motion; **ν**, stretching; **δ,** in plane bending; **γ**, out of plane bending; **ρ**, in plane rocking; **Δ**, in plane ring deformation; **Γ**: out of plane carbon skeleton deformation; **s**, symmetric; **as**, antisymmetric. A grey background is used to identify multiplets.

Table 7 Vibrational assignment of the TCT(OH) isomer of trifluoroacetylacetone in neon and *para*-hydrogen. Values for argon matrices from ref. [22] are also included. Calculated harmonic frequencies [M06-2X/6-311++G(3df,3pd)] (cm-1) are added for comparison. IR intensities (km/mol) are obtained in the harmonic approximation. Scaling factor (sf): 0.973; The complete set of calculated frequencies and intensities, as well as the corresponding assignments, is given in Table S8

Assignments (simplified description)	**Frequencies**				**Infrared Intensities**
	Experimental			**Theoretical Harmonic*sf**	
	Ne	**pH₂**	**Ar (ref.** [22]**)**		
νOH	3631.8	3612.8	3604	3756.8	177
νCH	3026.1	3014.8		3155.0	5
νCH₃	2983.2	2980.8		3099.6	6
νCH₃	2931.8	2929.7		3057.3	2
νCH₃		2902.3		2991.8	0.1
νC=O	1709.9	1709.5 1705.5	1710	1768.9	251
νC=C/ δOH	1697.2	1693.3	1693	1737.2	99
δCH₃	1435.8	1434.9	1436	1440.2	10
δCH₃	1424	1422.2	1421	1431.0	64
νC-O/νC-CF₃/δCH₃	1394.3	1394.3	1394	1405.2	96
δCH₃	1369	1367.4	1366	1364.0	46
δOH/ δCH	1306.1	1306.4	1305	1303.2	42
δOH/ νC-C	1249.4	1248.3	1259	1256.4	218
δCH/ νCF₃	1243.8	1242.6	1242	1242.7	183
νCF₃/νC(H)-C(=O)/ δCH₃	1221.2	1220.5	1217	1237.6	444
νCF₃	1146 1143.5	1142.3	1142	1164.7	281
δCH/νC-O/ ρCH₃/νCF₃	1076.8	1077.8	1078	1084.6	12
ρCH₃	1027.4	1026.4	1026	1024.9	7
ρCH₃/νC-O	995.4	995.0	996	989.8	32
γCH/Γ	858.1 856.2	856.3	855	868.9	31
νC-CF₃/ δC=C-C	850	851.1	852	856.5	25
νC-CH₃/ νC(H)-C(=O)	809.9	810.9	812	809.1	7

Δ	712.7	713.4	714	709.5	18
Γ				699.5	3

[a] main characteristic motion; **ν**, stretching; **δ,** in plane bending; **γ**, out of plane bending; **ρ**, in plane rocking; **Δ**, in plane ring deformation; **Γ**: out of plane carbon skeleton deformation; **s**, symmetric; **as**, antisymmetric. A grey background is used to identify multiplets.

It is important to point out that for the CCC and open enol isomers produced in F6-acac and F3-acac, the theoretical description of the frequency (and also the intensity) for the C-F stretching modes is not totally satisfactory, obtaining quite often more than 15-20 cm^{-1} shift from experimental values even after application of the scaling factor. These modes are not well reproduced within the frame of the level of theory used in this work, i.e., DFT/M06-2X calculations and harmonic approximation (the basis set is quite complete). A more complete test using different functionals and the MP2 method is performed on the CCC isomer and described in a forthcoming publication. We can advance that the description of these modes remains still poor compared to other modes. Kreienborg and Merten have previously investigated how M06-2X outperforms B3LYP in the harmonic description of C-F modes of two organic molecules in solution[28]. They found that this behavior is probably explained by error cancellation. In our case, the M06-2X also surpasses the B3LYP performance, but it is still not enough for a precise assignment. The clear vibrational data obtained in this work for different isomers of two analogues in cryogenic matrices can serve as a reference point for future benchmark developments in this sense.

4. Discussion

The UV laser irradiation experiments carried out for the set of molecules studied in the present and previous works can provide an updated general picture on how photoisomerization process takes place in the family of analogues of acetylacetone: acac (and deuterated isotopologues), F6-acac, F3-acac. The arguments used in this discussion are based on some of the seminal ideas given by Minoura *et al.* in their study about the photoisomerization of F3-acac in argon matrix [22], on the theoretical study done by Chen *et al.* [39], as well as on more recent experimental results [14, 15, 40, 41].(add ref 23(acacD2)

Previous studies of the photoisomerization process of acetylacetone suggest that the mechanism starts with the Franck-Condon excitation ($\pi \rightarrow \pi^*$) to the $S_2(\pi\pi^*)$ state [39]. The deexcitation pathway involves a decay to the $S_1(n\pi^*)$ state through vibronic interaction, which then relaxes to the $T_1(\pi\pi^*)$ state by means of an $S_1/T_1/T_2$ three-surface intersection. This picture has also been supported by the experimental works of Xu *et al.* [42], Poisson *et al.* [43] and Squibb *et al.* [40]. However, gas phase experiments also demonstrated that the dissociation channel is favored in this medium from the T_1 state [40]. Although the formation of the open enol isomers has been observed in liquid solutions [44],

only in cryogenic matrices these forms are stabilized and clearly observed. The calculations done by Chen *et al.* [39] also suggest that rotational isomerization can easily proceed in the $T_1(\pi\pi^*)$ state. According to their work, in this state, there is a rupture of the planar configuration in the pseudo-ring of the molecule, which does not occur in the other states [39]. These observations are also supported by the recent experimental work of Haugen et al. on F6-acac by using ultrafast X-ray transient absorption spectroscopy, indicating that multiple rotational isomers can be present in T_1 and possibly in S_1 as well [14].

The experimental data (UV spectra) and theoretical calculations obtained for the analogues of acetylacetone show that the excitation of the CCC isomer always proceeds as a $\pi \rightarrow \pi^*$ transition between S_0 and S_2 electronic levels. This sets a common starting point for the subsequent mechanism of relaxation. In addition, a similar deexcitation pathway has been found in acac and F6-acac [14]. Thus, a plausible hypothesis is that the mechanisms taking the systems from the $S_2(\pi\pi^*)$ excited state to the $T_1(\pi\pi^*)$ state where the isomerization takes place could be similar for all analogues under study.

As shown in several works on the different analogues, two main groups of open enol isomers are always formed after UV laser irradiation: CTZ (first group) and TCZ (second group) isomers [9, 22, 23, 45, 46]. The first group is mainly produced after irradiation of the CCC isomer at wavelengths between 270-310 nm. This range of excitation wavelengths is always on the onset of the CCC absorption band, which is the isomer with the lowest excitation energy in each analogue. By doing so we guarantee that this first excitation is almost totally selective to CCC, and that the newly formed isomers are not simultaneously excited (or very little). However, we have observed that the second group of isomers is also produced under these conditions, but in a much lower quantity. This second group is mainly observed when the first group is irradiated at lower wavelengths: 250-280 nm. A common characteristic of both groups is that the most stable isomer of each group is always observed. Indeed, the results obtained from the studies on the deuterated isotopologues of acetylacetone [23] and chloroacetylacetone [47] (to be published) have shown that after irradiation both isomers from the XYC-XYT produced pair are observed in their electronic ground state. Afterward, a conversion in the electronic ground state between the less stable and more stable isomers of each XYC-XYT pair occurs through the tunneling effect of the hydroxyl hydrogen [ref acacD2 (23)]. The kinetics of this process is very fast for the non-deuterated molecules which explains why only the most stable species of each XYC-XYT pair is observed at the end of the irradiation. A fast-tunneling process of the hydroxyl hydrogen in the CCT-CCC pair can also explains why the CCT isomer has never been observed, even in the case of hexafluoroacetylacetone where it is the most stable open enol isomer. This was one of the missing keys to understanding of the whole isomerization process in the acetylacetone family, which was originally envisaged by Minoura et al [22], and later demonstrated by our group [23]. It is

noteworthy that the change of orientation of an OH group under IR irradiation was observed in many molecules trapped in matrices and that tunneling and vibrational excitation could be entangled in conformational interconversions, as was demonstrated for example in ref [10.1021/acs.jpca.9b01382].

Overall, our studies combined with those of Nakata's group, suggest that the nature of the hosts used in these studies (argon, neon, nitrogen, and *para*-hydrogen) do not play a specific role in the relaxation mechanism. It means these matrices play mainly the role of a cold bath which takes part of the excess energy favoring the photoisomerization and avoiding photofragmentation. However, as observed for other systems, the interactions with the matrix can be important enough to block the tunneling effect in the ground state [38, 46–48]. This could explain the observation of the higher energy isomer of the TCT-TCC pair in acetylacetone, i.e. TCT, by Nagashima et al. in argon matrix [45] and by our group in normal hydrogen (nH_2) [49]. The observation of this specific isomer, in comparison with the non-observation of CTT (the less stable isomer in the CTZ pair) remains unclear . Considering that the height and the width of the isomerization barriers are very similar in both pairs (TCT-TCC and CTT-CTC) [23, 47], neither different tunneling kinetics nor different vibrational excitation can explain the observed behavior.

The experimental and theoretical results allow explaining some of the steps in the formation of the two groups of open isomers. First, experiments show that it is more probable to produce CTZ isomers after excitation of CCC (whatever the irradiation wavelength in the UV absorption of CCC) than TCZ and TTZ isomers. Several arguments can be used to explain the formation of the first group (CTZ isomers). In the $T_1(\pi\pi^*)$ state of the CCC isomer for all the analogs, the C_2-C_3 bond has a single bond character [39]. This can also have two implications: first, an increase of C_2-C_3 bond distance, and second, the loss of the π electronic conjugation. Both effects impact the intramolecular hydrogen bond present in the CCC isomer, lowering its strength. The weakening of this hydrogen bond and the C_2-C_3 bond will favor the rotation around the latter allowing the formation of isomers of the type XTZ. We should remark that the probability of forming TTZ isomers is usually very low because repulsive steric effects are present, being then CTZ the main product. In the present study, we effectively observed the formation of CTT (under irradiation of F6-acac) and CTC(CO) (under irradiation of F3-acac – CCC(CO)) as the first steps in photoisomerization.

In the case of the second group (TYZ), the experimental evidence, thanks to tunable UV excitation, indicates that the isomers are mainly formed by irradiation (250-280 nm) of the first group of isomers (CTZ). They are in fact also formed as minor products directly from CCC as proved by kinetics studies on acac [49]. Like in the case of CCC, the excitation of CTZ isomers proceeds via a $\pi \rightarrow \pi^*$ excitation ($S_2 \leftarrow S_0$), but at a higher energy. The excitation could be followed by relaxation in the T_1 state, weakening the C=C double bond, like in CCC. Then, the system can return either to a CCZ configuration

(producing at the end CCC) or to TCZ isomers. The production of TCZ isomers should be less probable because two bonds need to be rotated. However, an internal energy excess due to higher excitation energy, and a lower barrier for C_1-C_2, could explain the rotation around the C_1-C_2bond. Even if the produced amount was small, these isomers absorb at lower wavelengths compared to CCC, and generally CTZ (Table S9 and S10), being in the end a stable final product. Under irradiation with wavelengths exciting CTZ, CCC is usually also excited (broad absorption band) and can react, whereas TCZ may be weakly excited. Then, even if the production channel to TCZ has a small probability, once the isomer is formed it does not return to the initial isomers (CTZ and CCC), which will then be depleted over time (or reach an equilibrium amount). This provokes in the end an accumulation of TCZ under such conditions. This scheme, following the kinetic study of acac [23, 49] and the conclusions of D2-acac irradiation study [23], is in full agreement with the present results of the UV photoisomerisation of F6-acac. We found a narrow range of UV irradiation leading to the detection of TCC in F6-acac samples. It should correspond to UV frequencies exciting much more efficiently CCC and CTT than TCC. TD-DFT calculations effectively indicate that this range should be narrow (see Table S9). We have not been able to detect TCC(CO) in the UV irradiation of F3-acac. TD-DFT calculations show that $\pi \rightarrow \pi^*$ transitions of TCC(CO) and CTC(CO) occur at the same energies (see Table S10), leading to an even narrower UV window to let TCC(CO) detectable that, probably, we haven't explored. On the other hand, TCC (F6-acac) was more difficult to detect than TCC (acac) under various UV irradiations even though TCC and CTC have very close UV absorption spectra in acac [23]. Nagashima et al. suggest that TYZ→CYZ can occur in the thermal relaxation in the ground state of F6-acac because of a floppy C-C bond. Taking this assumption in mind, the present results agree with a low rotational barrier around the C_1-C_2 bond of the carbonated skeleton with CF_3 on the C=O side of the acetylacetone derivative. Moreover, irradiation of the open enol isomers in all analogues at lower wavelengths can also take back the system to the CCC isomer. This experimental fact actually agrees with the previous mechanism scheme. When open enol isomers are excited at lower wavelengths, they can produce several new isomers, most of them absorbing in the same spectral region, except the CCC isomer, that in all cases presents a very well-separated and redshifted absorption band. Accordingly, CCC accumulates very efficiently as a function of irradiation time. Thus, the experimental data support the idea that multiple configurational and conformational minima are explored during the time these systems spend in the excited and ground state.

However, other processes can also take place during the excited state dynamics and explain the CTZ→TCZ conversion [22]. This is illustrated by the interesting case of trifluoroacetylacetone. The asymmetry of the molecule helps to demonstrate that after UV excitation, intramolecular hydrogen transfer can occur in the excited state, as experimentally observed in the production of its different

open enol isomers. This is particularly true for the CTZ→TCZ conversion, where the passage of a hydrogen atom from the hydroxyl group to the carbonyl group can directly produce the expected conversion. The non-planar geometries at play in the $T_1(\pi\pi^*)$ state together with a weakening of the C_2=C_3 bond can favor the approach of the groups with oxygen atoms and the subsequently intramolecular hydrogen transfer. UV-induced intramolecular H-transfers were previously observed in several systems isolated in matrices, e.g. refs http://dx.doi.org/10.1039/c0cp02812f or http://dx.doi.org/10.1021/jp2059563, explained by a radicalar mechanism with migration of a labile hydrogen in the relaxation process involving a dissociative S_1 ($\pi\sigma^*$) state [ref Sobolewski]. Such a process can be discarded in the case of the acetylacetone analogs under study because $\pi\sigma^*$ states lie at higher energies (see Table S9 and S10) and S_1 is a $n\pi^*$ state, without evident weakening of the O-H bond. Moreover, the non-observation of photo-produced radicals in parahydrogen matrices weakens in fact the possibility of a radicalar mechanism (see below). In the case of F3-acac, the pathway involving an H-transfer in the excited states could be also more efficient than that leading to the formation of TCZ(CO) isomers from CCC or CTC(CO) under UV irradiation, lowering the possibility to detect TCC(CO). As expected, only the isomers of lower energies in the XYT(OH)-XYC(OH) are observed: CTT(OH) and TCT(OH). These two isomers absorb at higher energies than CTC(CO) and CCC(CO) following the TD-DFT estimations, and thus their produced amount is not affected by subsequent UV irradiations when exciting CTC(CO) or CCC(CO). Moreover, CTT(OH) and TCT(OH) have quite distinct $\pi \rightarrow \pi^*$ transition energies from TD-DFT predictions, allowing their production in different amounts depending on the UV irradiation wavelength. We remark that with the current knowledge, it remains still uncertain whether the hydrogen atom transfer process in the excited state or the "accumulative scheme" described in the previous paragraph prevails one over the other in the different isomers and excitation energies in the production of TCZ isomers. However, an H-transfer in the excited states is also an assumption in agreement with the fact that after a sequence of UV irradiations to come back to CCC through the formation of XYT(OH) isomers, the final [CCC(CO)]/[CCC(OH)] ratio was found larger than the initial one in nitrogen matrices [20 -TFacac].

It is important to note that in all the systems after the UV excitation of the CCC isomer at wavelengths between 290-310 nm, almost no fragments were detected. If instead of direct isomerization, a recombination process takes place to form enolic isomers, it is very likely that we will observe some escaping fragments in *para*-hydrogen matrix, thanks to the softness of this matrix. The experimental evidence disfavors this mechanism. Nevertheless, at lower wavelengths, bands from fragments start to grow (e.g., CO product is clearly observed), which indicates an opening of these channels under such energetic conditions. These results support and enlarge the initial hypothesis stating that under a certain range of energy in the two systems under study, the matrix mainly plays the role of a cold bath

dissipating a part of the excess energy and diminishing the probability to lead the systems to fragmentation channels.

5. Conclusions

We have revisited the photoisomerization process induced by UV laser selective excitation in hexafluoroacetylacetone and trifluoroacetylacetone. New vibrational and electronic spectroscopic data of the chelated and open enol isomers of the halogenated analogues of acetylacetone in neon and *para*-hydrogen matrices were obtained. These new data allow us to perform a careful assignment of most of the infrared bands of the produced open enol isomers in F6-acac and F3-acac analogues. At the same time, the results provide new clear experimental vibrational frequencies of C-F stretching modes that can be used to improve the current theoretical approaches to describe these modes, which are still not properly reproduced. We also obtained for the first time the electronic absorption spectrum for the chelated enol isomer, as well as for the open enol isomers CTT(OH) and TCT(OH) of F3-acac. The comparison with theoretical TD-DFT calculations supports the assignment.

We have shown that a very similar set of isomers is obtained in the soft matrices (Ne and pH_2) with selective UV excitation compared to those obtained by Nakata's group in argon matrix with broadband UV excitation, i.e., CTT for F6-acac [9], and CTC(CO), CTT(OH), and TCT(OH) for F3-acac [22]. However, in the case of F6-acac, a new isomer (TCC) was observed under a very narrow excitation window, which was explained by experimental UV absorption experiments and TD-DFT calculations. Overall, the main results concerning the photoisomerization process of F6-acac and F3-acac in the studied matrices can be summarized as follows: (i) TTT and TTC isomers (in both analogs) are not produced because of their high relative energy due to destabilizing repulsive interactions; (ii) intramolecular hydrogen transfer can occur in the electronic excited states; and (iii) if the UV irradiation produces one of the isomers of the pairs CTC-CTT or TCT-TCC, the system always ends in the most stable isomer of the pair in the ground state. These three points can explain the final production of most of the observed isomers in argon, neon, and *para*-hydrogen, where interactions with the host are small. Nevertheless, preliminary experiments in nitrogen matrices seem to show the same result. Studies in more interacting matrices (e.g., normal hydrogen) could also be useful in this sense. Deeper studies based on the effect of the UV irradiation wavelength on photoisomerization are necessary to explain the complex processes at play in the relaxation of F3-acac, and to conclude the possibility to produce the TCC(CO) isomer in F3-acac. Finally, theoretical calculations could be very helpful to understand some of the missing or incomplete points of the photodynamics of these systems. In particular, the theoretical study of the excited state hydrogen transfer process taking place in these systems (at least experimentally proved on F3-acac) is of great interest. These results highlight the use of UV photoisomerization in matrices as a probe of molecular internal processes.

Acknowledgments

We acknowledge the use of the high-performance computing center MésoLUM managed by ISMO (UMR8214) and LPGP (UMR8578), University Paris-Saclay (France). This work was supported by the RTRA Triangle de la Physique (2013-0436T REACMAQ). It benefited from the French-Lithuanian PHC GILIBERT program (42125XF and S-LZ-19−1 from RCL) and the French-Cuban PHC Carlos Finlay program (41805NA).

Data Availability Statement

This article has data included as electronic supplementary information. Additional data will be made available on reasonable request.

Author contribution statement

C.C., M.C., J.C. and A.G.Q. contributed to the study conception and design. All authors were involved in material preparation, data collection, and analysis. The first draft of the manuscript was written by A.G.Q. and all authors contributed to the production of subsequent versions of the manuscript. All authors read and approved the final manuscript.

References

1. Andreassen AL, Zebelman D, Bauer SH (1971) Hexafluoroacetylacetone and hexafluoroacetic anhydride. J Am Chem Soc 93:1148–1152. https://doi.org/10.1021/ja00734a020
2. Iijima K, Tanaka Y, Onuma S (1992) Internal rotation of trifluoromethyl groups in hexafluoroacetylacetone. J Mol Struct 268:315–318. https://doi.org/10.1016/0022-2860(92)85081-Q
3. Evangelisti L, Tang S, Velino B, et al (2009) Hexafluoroacetylacetone: A 'rigid' molecule with an enolic Cs shape. Chem Phys Lett 473:247–250. https://doi.org/10.1016/j.cplett.2009.03.080
4. Burk P, Koppel IA (1993) An AM1 and PM3 study of hexafluoroacetylacetone. Journal of Molecular Structure: THEOCHEM 282:277–282. https://doi.org/10.1016/0166-1280(93)85012-N

5. Buemi G (2000) Ab initio DFT study of the hydrogen bridges in hexafluoro-acetylacetone, trifluoro-acetylacetone and some 3-substituted derivatives. Journal of Molecular Structure: THEOCHEM 499:21–34. https://doi.org/10.1016/S0166-1280(99)00265-1

6. Chatterjee C, Incarvito CD, Burns LA, Vaccaro PH (2010) Electronic structure and proton transfer in ground-state hexafluoroacetylacetone. Journal of Physical Chemistry A 114:6630–6640. https://doi.org/10.1021/jp101224e

7. Tayyari SF, Zeegers-Huyskens Th, Wood JLL (1979) Spectroscopic study of hydrogen bonding in the enol form of β-diketones-I. Vibrational assignment and strength of the bond. Spectrochim Acta A 35A:1265–1275. https://doi.org/10.1016/0584-8539(79)80208-1

8. Nakanishi H, Morita H, Nagakura S (1978) Charge-Transfer Character in the Intramolecular Hydrogen Bond: Vacuum Ultraviolet Spectra of Acetylacetone and Its Fluoro Derivatives. Bull Chem Soc Jpn 51:1723–1729. https://doi.org/10.1246/bcsj.51.1723

9. Nagashima N, Kudoh S, Nakata M (2003) Infrared and UV-visible absorption spectra of hexafluoroacetylacetone in a low-temperature argon matrix. I. Structure of a non-chelated enol-type isomer. Chem Phys Lett 374:59–66. https://doi.org/10.1016/S0009-2614(03)00688-2

10. Nagashima N, Kudoh S, Nakata M (2003) Infrared and UV-visible absorption spectra of hexafluoroacetylacetone in a low-temperature argon matrix. II. Detection of the nπ* transition by monitoring IR spectral changes due to photoisomerization. Chem Phys Lett 374:67–73. https://doi.org/10.1016/S0009-2614(03)00689-4

11. Bassett JE, Whittle E (1976) The photochemistry of hexafluoroacetylacetone in the vapour phase. Occurrence of a novel HF elimination reaction. Int J Chem Kinet 8:859–876. https://doi.org/10.1002/kin.550080606

12. Yoon M-C, Choi YS, Kim SK (1999) Photodissociation dynamics of acetylacetone: The OH product state distribution. J Chem Phys 110:11850. https://doi.org/10.1063/1.479126

13. Muyskens KJ, Alsum JR, Thielke TA, et al (2012) Photochemistry of UV-excited trifluoroacetylacetone and hexafluoroacetylacetone I: Infrared spectra of fluorinated methylfuranones formed by HF photoelimination. Journal of Physical Chemistry A 116:12305–12313. https://doi.org/10.1021/jp307725z

14. Haugen EA, Hait D, Scutelnic V, et al (2023) Ultrafast X-ray Spectroscopy of Intersystem Crossing in Hexafluoroacetylacetone: Chromophore Photophysics and Spectral Changes in the Face of

Electron-Withdrawing Groups. J Phys Chem A 127:634–644. https://doi.org/10.1021/acs.jpca.2c06044

15. Bhattacherjee A, Pemmaraju C Das, Schnorr K, et al (2017) Ultrafast Intersystem Crossing in Acetylacetone via Femtosecond X-ray Transient Absorption at the Carbon K-Edge. J Am Chem Soc 139:16576–16583. https://doi.org/10.1021/jacs.7b07532

16. Gordon MS, Koob RD (1973) An INDO Investigation of the Structure and Bonding of Acetylacetone and Trifluoroacetylacetone. J Am Chem Soc 433:5863–5867

17. Raissi H, Nowroozi A, Roozbeh M, Farzad F (2006) Molecular structure and vibrational assignment of (trifluoroacetyl) acetone: A density functional study. J Mol Struct 787:148–162. https://doi.org/10.1016/j.molstruc.2005.10.042

18. Favero LB, Evangelisti L, Velino B, Caminati W (2014) Morphing the Internal Dynamics of Acetylacetone by $CH_3 \rightarrow CF_3$ Substitutions. The Rotational Spectrum of Trifluoroacetylacetone. J Phys Chem A 118:4243–4248. https://doi.org/10.1021/jp5005727

19. Sliznev V V, Lapshina SB, Girichev G V (2002) Ab Initio Structure Investigation of the Enol Forms of β-Diketones RCOCH2COR (R = H, CH3, CF3). Journal of Structural Chemistry 43:47–55. https://doi.org/10.1023/A:1016065614664

20. Gutiérrez-Quintanilla A, Platakyte R, Chevalier M, et al (2021) Hidden Isomer of Trifluoroacetylacetone Revealed by Matrix Isolation Infrared and Raman Spectroscopy. J Phys Chem A 125:2249–2266. https://doi.org/10.1021/acs.jpca.0c10945

21. Zahedi-Tabrizi M, Tayyari F, Moosavi-Tekyeh Z, et al (2006) Structure and vibrational assignment of the enol form of 1,1,1-trifluoro-2,4-pentanedione. Spectrochim Acta A Mol Biomol Spectrosc 65:387–396. https://doi.org/10.1016/j.saa.2005.11.019

22. Minoura Y, Nagashima N, Kudoh S, Nakata M (2004) Mechanism of UV-Induced Conformational Changes among Enol-Type Isomers of (Trifluoroacetyl)acetone Studied by Low-Temperature Matrix-Isolation Infrared Spectroscopy and Density Functional Theory Calculation. J Phys Chem A 108:2353–2362. https://doi.org/10.1021/jp031192y

23. Gutiérrez-Quintanilla A, Chevalier M, Crépin C (2016) Double deuterated acetylacetone in neon matrices: infrared spectroscopy, photoreactivity and the tunneling process. Physical Chemistry Chemical Physics 18:20713–20725. https://doi.org/10.1039/C6CP02796B

24. Frisch MJ, Trucks GW, Schlegel HB, et al (2009) Gaussian 09 Revision D.01

25. Becke AD (1993) Density-functional thermochemistry. III. The role of exact exchange. J Chem Phys 98:5648. https://doi.org/10.1063/1.464913

26. Zhao Y, Truhlar DG (2008) The M06 suite of density functionals for main group thermochemistry, thermochemical kinetics, noncovalent interactions, excited states, and transition elements: Two new functionals and systematic testing of four M06-class functionals and 12 other function. Theor Chem Acc 120:215–241. https://doi.org/10.1007/s00214-007-0310-x

27. Krishnan R, Binkley JS, Seeger R, Pople JA (2008) Self-consistent molecular orbital methods. XX. A basis set for correlated wave functions. J Chem Phys 72:650–654. https://doi.org/10.1063/1.438955

28. Kreienborg NM, Merten C (2019) How to treat C–F stretching vibrations? A vibrational CD study on chiral fluorinated molecules. Phys Chem Chem Phys 21:3506–3511. https://doi.org/10.1039/C8CP02395F

29. Runge E, Gross EKU (1984) Density-Functional Theory for Time-Dependent Systems. Phys Rev Lett 52:997–1000. https://doi.org/10.1103/PhysRevLett.52.997

30. Bauernschmitt R, Ahlrichs R (1996) Treatment of electronic excitations within the adiabatic approximation of time dependent density functional theory. Chem Phys Lett 256:454–464. https://doi.org/https://doi.org/10.1016/0009-2614(96)00440-X

31. Casida ME, Jamorski C, Casida KC, Salahub DR (1998) Molecular excitation energies to high-lying bound states from time-dependent density-functional response theory: Characterization and correction of the time-dependent local density approximation ionization threshold. J Chem Phys 108:4439–4449. https://doi.org/10.1063/1.475855

32. Frisch MJ, Trucks GW, Schlegel HB, et al (2016) Gaussian 16 Revision B.01

33. Johnson ER, Keinan S, Mori-Sánchez P, et al (2010) Revealing Noncovalent Interactions. J Am Chem Soc 132:6498–6506. https://doi.org/10.1021/ja100936w

34. Contreras-García J, Johnson ER, Keinan S, et al (2011) NCIPLOT: A Program for Plotting Noncovalent Interaction Regions. J Chem Theory Comput 7:625–632. https://doi.org/10.1021/ct100641a

35. Humphrey W, Dalke A, Schulten K (1996) VMD: Visual molecular dynamics. J Mol Graph 14:33–38. https://doi.org/10.1016/0263-7855(96)00018-5

36. Tayyari SF, Najafi A, Afzali R, et al (2008) Structure and vibrational assignment of the enol form of 1-chloro-1,1-difluoro-pentane-2,4-dione. J Mol Struct 878:10–21. https://doi.org/https://doi.org/10.1016/j.molstruc.2007.07.040

37. Nowroozi A, Roohi H, Sadeghi Ghoogheri MS, Sheibaninia M (2011) The competition between the intramolecular hydrogen bond and π-electron delocalization in trifluoroacetylacetone-A theoretical study. Int J Quantum Chem 111:578–585. https://doi.org/10.1002/qua.22129

38. Trivella A, Roubin P, Theulé P, et al (2007) UV and IR Photoisomerization of Acetylacetone Trapped in a Nitrogen Matrix. J Phys Chem A 111:3074–3081. https://doi.org/10.1021/jp068763h

39. Chen X-B, Fang W-H, Phillips DL (2006) Theoretical Studies of the Photochemical Dynamics of Acetylacetone: Isomerzation, Dissociation, and Dehydration Reactions. J Phys Chem A 110:4434–4441. https://doi.org/10.1021/jp057306i

40. Squibb RJ, Sapunar M, Ponzi A, et al (2018) Acetylacetone photodynamics at a seeded free-electron laser. Nat Commun 9:63. https://doi.org/10.1038/s41467-017-02478-0

41. Trivella A, Wassermann TN, Mestdagh JM, et al (2010) New insights into the photodynamics of acetylacetone: isomerization and fragmentation in low-temperature matrixes. Physical Chemistry Chemical Physics 12:8300. https://doi.org/10.1039/c003593a

42. Xu S, Park ST, Feenstra JS, et al (2004) Ultrafast electron diffraction: Structural dynamics of the elimination reaction of acetylacetone. Journal of Physical Chemistry A 108:6650–6655. https://doi.org/10.1021/jp0403689

43. Poisson L, Roubin P, Coussan S, et al (2008) Ultrafast dynamics of acetylacetone (2,4-pentanedione) in the S2 state. J Am Chem Soc 130:2974–2983. https://doi.org/10.1021/ja0730819

44. Verma PK, Koch F, Steinbacher A, et al (2014) Ultrafast UV-Induced Photoisomerization of Intramolecularly H-Bonded Symmetric β-Diketones. J Am Chem Soc 136:14981–14989. https://doi.org/10.1021/ja508059p

45. Nagashima N, Kudoh S, Takayanagi M, Nakata M (2001) UV-Induced Photoisomerization of Acetylacetone and Identification of Less-Stable Isomers by Low-Temperature Matrix-Isolation Infrared Spectroscopy and Density Functional Theory Calculation. J Phys Chem A 105:10832–10838. https://doi.org/10.1021/jp012557m

46. Trivella A, Coussan S, Chiavassa T, et al (2006) Comparative study of structure and photo-induced reactivity of malonaldehyde and acetylacetone isolated in nitrogen matrices. Low Temperature Physics 32:1042–1049. https://doi.org/10.1063/1.2389011

47. Gutiérrez Quintanilla A (2016) Molecules and complexes with hydrogen bond: solvation and photoreactivity in cryogenic matrices. Université de Paris-Saclay

48. Gutiérrez-Quintanilla A, Chevalier M, Platakyte R, et al (2020) Intramolecular hydrogen tunneling in 2-chloromalonaldehyde trapped in solid para -hydrogen. Physical Chemistry Chemical Physics 22:6115–6121. https://doi.org/10.1039/C9CP06866J

49. Lozada-García RR, Ceponkus J, Chevalier M, et al (2012) Photochemistry of acetylacetone isolated in parahydrogen matrices upon 266 nm irradiation. Phys Chem Chem Phys 14:3450. https://doi.org/10.1039/c2cp23913b